

LARGE SCALE FINITE ELEMENT THERMAL ANALYSIS OF THE BOLTS OF A FRENCH PWR CORE INTERNAL BAFFLE STRUCTURE

ISABELLE RUPP*, CHRISTOPHE PÉNIGUEL and MICHEL TOMMY-MARTIN¹

EDF R&D, 6 quai Watier, 78401 Chatou France

¹ 1 av du Général de Gaulle, Clamart 92141 France

*Corresponding author. E-mail : isabelle.rupp@edf.fr

Received January 12, 2009

Accepted May 15, 2009

The internal core baffle structure of a French Pressurized Water Reactor (PWR) consists of a collection of baffles and formers that are attached to the barrel. The connections are done thanks to a large number of bolts (about 1500). After inspection, some of the bolts have been found cracked. This has been attributed to the Irradiation Assisted Stress Corrosion Cracking (IASCC). The Electricité De France (EDF) has set up a research program to gain better knowledge of the temperature distribution, which may affect the bolts and the whole structure. The temperature distribution in the structure was calculated thanks to the thermal code SYRTHES that used a finite element approach. The heat transfer between the by-pass flow inside the cavities of the core baffle and the structure was accounted for thanks to a strong thermal coupling between the thermal code SYRTHES and the CFD code named *Code_Saturne*.

The results for the CP0 plant design show that both the high temperature and strong temperature gradients could potentially induce mechanical stresses. The CPY design, where each bolt is individually cooled, had led to a reduction of temperatures inside the structures.

A new parallel version of SYRTHES, for calculations on very large meshes and based on MPI, has been developed. A demonstration test on the complete structure that has led to about 1.1 billion linear tetraedra has been calculated on 2048 processors of the EDF Blue Gene computer.

KEYWORDS : Thermal Hydraulics, Internal Core Baffle, Conjugate Heat Transfer, Parallelization

1. INTRODUCTION

The internal core baffle structure of a PWR ensures the transition between the polygonal core contour and the circular shape of the core barrel. It also helps in protecting the main vessel from the neutron effect (Figure 1).

The internal core baffle structure consists of vertical baffles and horizontal formers that are attached to the barrel (Figure 2). Each baffle being independent, the connection between the core baffle sheets, the formers, and the core barrel is done thanks to a large number of bolts (about 1500). Indeed, a precise positioning is required since the baffles are just a few mm away from the fuel assemblies.

Due to the proximity of the core, a strong internal energy deposition induced by gamma radiation has affected the internal baffle structure. A cooling by a by-pass flow has therefore been introduced during the design phase of the nuclear plant. In 1987, EDF decided to control (with Ultra Sonic technique) the bolts tightening, the formers,

and the baffles of the Bugey 2 nuclear plant. A certain number of bolts were found cracked. After destructive investigations in the EDF hot cells of some removed bolts, the cracking phenomenon was attributed to the Irradiation Assisted Corrosion (IASCC) [1]. Recently, EDF has created a research program to get better knowledge of the temperature distribution that is affecting these bolts. Indeed, temperature is one of the factors of the IASCC phenomenon. Calculations have been done on 900 MW plants with a configuration named CP0 (see [2]) where the correlation between the damage observed on site and the temperature reached was confirmed. Moreover, the temperature is a needed input for the functional analysis that is aimed at determining the stress and strain of the whole internal structures during operation. A new, more complex calculation has been started for 900 MW plants with a configuration named CPY in order to prove that the new design of the baffle should reduce a lot of the temperature loads seen by the bolts.

As shown in Figure 3, the CPY geometry to handle is

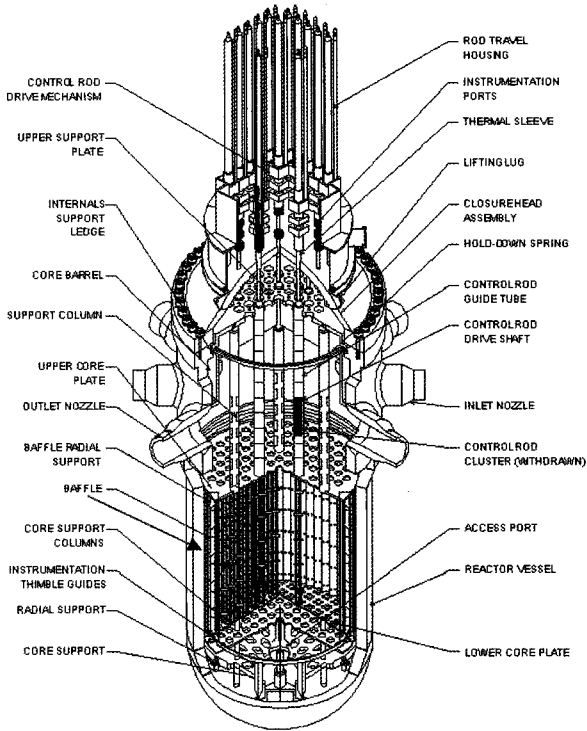


Fig. 1. General View of a PWR Vessel and the Baffle Location in the Reactor

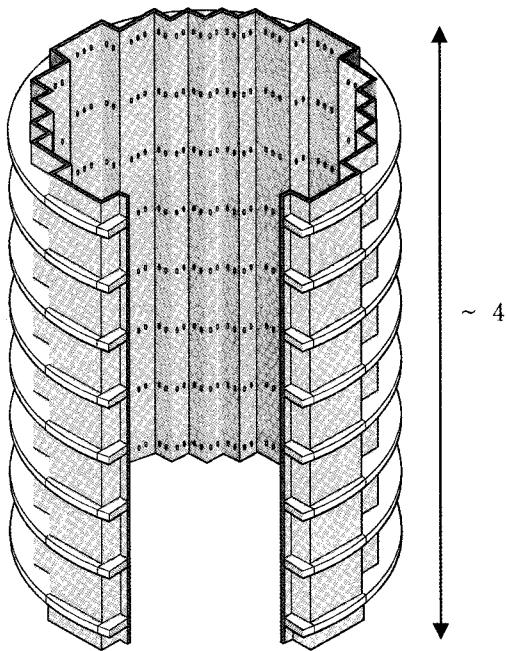


Fig. 2. Baffle (Vertical Sheets)

more complex due to the presence of individual cooling passages around most of the bolts located near the core. Experimental approaches have been used in the past.

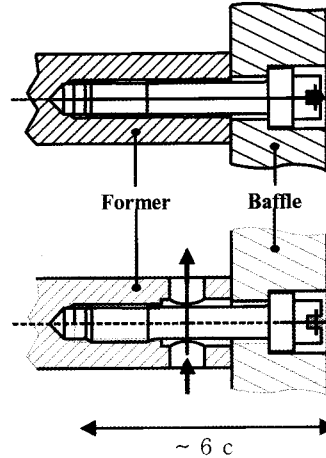


Fig. 3. Details of the Bolts – Introduction of Individual Cooling Passages for the CPY Reactor

but they became quite costly when they were dealing with such a high temperature, pressure, and potentially dangerous environments (as is the case for the present nuclear component). Moreover, on site experimental approaches often lack the flexibility needed when a sensitivity study is desired. On the other hand, affordable powerful computer facilities are now at our disposal at EDF and they look promising in handling these kinds of problems. This paper describes the numerical procedure that was followed to accurately calculate the temperature distribution inside the core baffle structure, including all of the bolts' details, and will focus on the new parallel version of the solid thermal code.

2. NUMERICAL APPROACH OF THE THERMAL PHENOMENA

In order to study numerically the damage potentially seen by the bolts, four numerical tools are currently used at EDF:

- The first one is a code that is able to calculate the three dimensional distribution of the neutron flux and the heat deposition due to the gamma radiation and neutrons. This is achieved with the Monte-Carlo Code TRIPOLI (developed by the Commissariat à l'Énergie Atomique, (CEA)). The purpose of this paper is not to describe the procedure. Details can be found in (Lee Y.K et al 2001),
- A Computational Fluid Dynamics (CFD) code that is able to compute the flow inside the cavities and the heat exchange at the wall. This is done thanks to the finite volume code *Code_Saturne* that was developed at EDF. For the last few years, there has been considerable effort in making this CFD code well adapted to parallel architectures,

- A solid thermal code, SYRTHES, that is able to take into account both the three dimensional heat deposition (provided by the TRIPOLI calculations) and the cooling effect (calculated by the *Code_Saturne*) that was induced by the by-pass flow. The last part of this paper is devoted to present a new parallel version of this code that is able to handle a large number of meshes,
- Finally, a mechanical code, *Code_Aster*, also developed at EDF, which takes into account the neutronic flux, as well as the fine temperature distributions, is used to estimate the mechanical behavior of the structure. It requires both a global and a very fine local temperature distribution provided by SYRTHES to be able to focus on different locations, particularly around each bolt. Again, for the time being, no feedback between the mechanical stresses calculations and the neutronic or thermal calculations is required. It is not the purpose of this paper to describe this part in detail.

In the present calculation the feedback between the neutron calculation and the thermal distribution is not taken into account (i.e. the temperature distribution found is not used to iteratively modify the neutron calculation) but the strong coupling between the CFD code and the solid thermal code is accounted for. Indeed, the flow temperature increases progressively as it removes heat when it flows upwards along the walls, cavities, and individual cooling passages.

2.1 In the Fluid – the CFD Code *Code_Saturne*

The EDF finite volume CFD code, *Code_Saturne*, is used to solve Navier-Stokes equations on unstructured meshes. The flow is assumed to be Newtonian and the density is only a function of temperature. The averaged Navier-Stokes equations can be written (the filtering operator that is used is omitted for the sake of clarity) :

$$\frac{\partial \rho}{\partial t} + \frac{\partial \rho U_j}{\partial x_j} = 0 \quad (1)$$

$$\rho \frac{\partial U_i}{\partial t} + \rho U_j \frac{\partial U_i}{\partial x_j} = -\frac{\partial p^*}{\partial x_i} + \frac{\partial}{\partial x_j} \left[\mu_e \left(\frac{\partial U_i}{\partial x_j} + \frac{\partial U_j}{\partial x_i} \right) \right] - \frac{2}{3} \frac{\partial}{\partial x_i} \left(\mu_e \frac{\partial U_i}{\partial x_j} \right) + (\rho - \rho_0) g_i \quad (2)$$

In Eq. 1 and 2, U_i are the filtered components of the velocity, p^* stands for the pressure (minus the reference hydrostatic pressure), μ_e represents $\mu + \mu_t$ where μ and μ_t are respectively the molecular and turbulent viscosities. Turbulence is handled through a classical k- ϵ model. More details on *Code_Saturne* can be found in [3,4].

In the collocated finite volume approach that is used in *Code_Saturne*, all variables are located at the centres of gravity of the cells (which may take any shape). The momentum equations are solved by considering an explicit

mass flux (the three components of the velocity are thus uncoupled). Velocity and pressure coupling is insured by a prediction/correction method with a SIMPLEC algorithm [5]. The Poisson equation is solved with a conjugate gradient method. The collocated discretization requires a Rhie and Chow [6] interpolation in the correction step in order to avoid any oscillatory solutions.

2.2 Conduction in the Solid – Code SYRTHES

The thermal solid code SYRTHES relies on a finite element technique to solve the general heat equation where all properties can be time, space, or temperature dependent.

$$\rho C_p \frac{\partial T}{\partial t} = \frac{\partial}{\partial x_j} \left(k_s \frac{\partial T}{\partial x_j} \right) + \Phi_v \quad (3)$$

In Eq. 3, T is the temperature, t the time, Φ_v a volume heat source or sink, and ρ and C_p , represent respectively the density and the specific heat. k_s (a matrix when the material is anisotropic) designates the conductive behaviour of the medium. For optimisation reasons, only two kinds of elements have been retained (triangles in 2D, tetrahedra in 3D). More details on the possibilities of the finite element code SYRTHES can be found in [7] and [8]. SYRTHES has been checked thoroughly against experimental and analytical test cases.

2.3 Heat Transfer at the Fluid/Solid Interface

At the interface, for each time step, the thermal coupling is performed. This coupling relies on an iterative procedure. Let T_s be the temperature of an internal solid node, T_w the temperature at a node that belongs to the interface, and T_f the temperature of a fluid point (located generally in the log layer). At time $t^{(n)}$, the CFD tool *Code_Saturne* provides after calculation:

- $h^{(n)}$: the local heat exchange coefficient at time $t^{(n)}$
- $T_f^{(n)}$: the local inside fluid temperature at time $t^{(n)}$

These quantities are calculated thanks to classical log law wall functions. The model is based on a 3-layer modeling. More detailed information can be found in [3].

Using these data, the flux to be applied to the solid is:

$$\varphi_s^{(n+1)} = h^{(n)} \left(T_w^{(n+1)} - T_f^{(n)} \right) \quad (4)$$

Then, using this flux or the exchange conditions $h^{(n)}$ and $T_f^{(n)}$, SYRTHES can solve the heat conduction equation inside the solid. This gives us an updated temperature for the entire solid region. These new values $T_s^{(n+1)}$, are also updated on the boundary. Therefore, $T_w^{(n+1)}$ is also known and the iterative procedure may keep going on.

3. CONFIGURATION SIMULATED

For the coupled calculation, due to symmetry reasons and limitation at that time in the thermal code (scalar

Table 1. Physical Properties of the Baffle and Formers

T(°C)	λ (W/m/°C)	ρC_p (J/m ³ /°C)
250	18.	4 265 402
300	18.6	4 295 612
350	19.3	4 346 846
400	20.	4 385 964

Table 2. Physical Properties of the Bolts

T(°C)	λ (W/m/°C)	ρC_p (J/m ³ /°C)
250	17.3	4 261 083
300	17.9	4 292 565
350	18.6	4 366 197
400	19.2	4 393 592

version), a limited sector of 45° was considered (even though the last part of this paper emphasizes that now the full domain could be tackled both by *Code_Saturne* and *SYRTHES*).

The material properties of the different parts are temperature dependent. They are given in Table 1 and Table 2.

Heat exchange boundary conditions are imposed on the external walls (core side of the baffle and the external wall of the core barrel). The inlet fluid temperature and by-pass flow rate are set respectively to 286 °C (the nominal

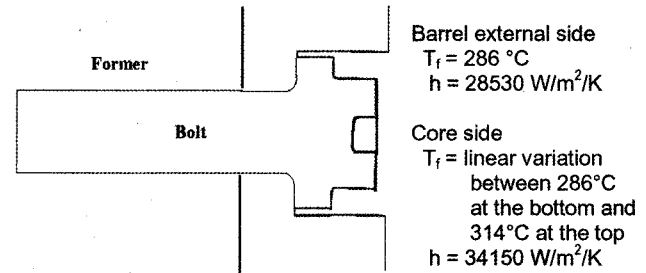


Fig. 4. Sketch of the Boundary Conditions Applied to the Bolts' Head

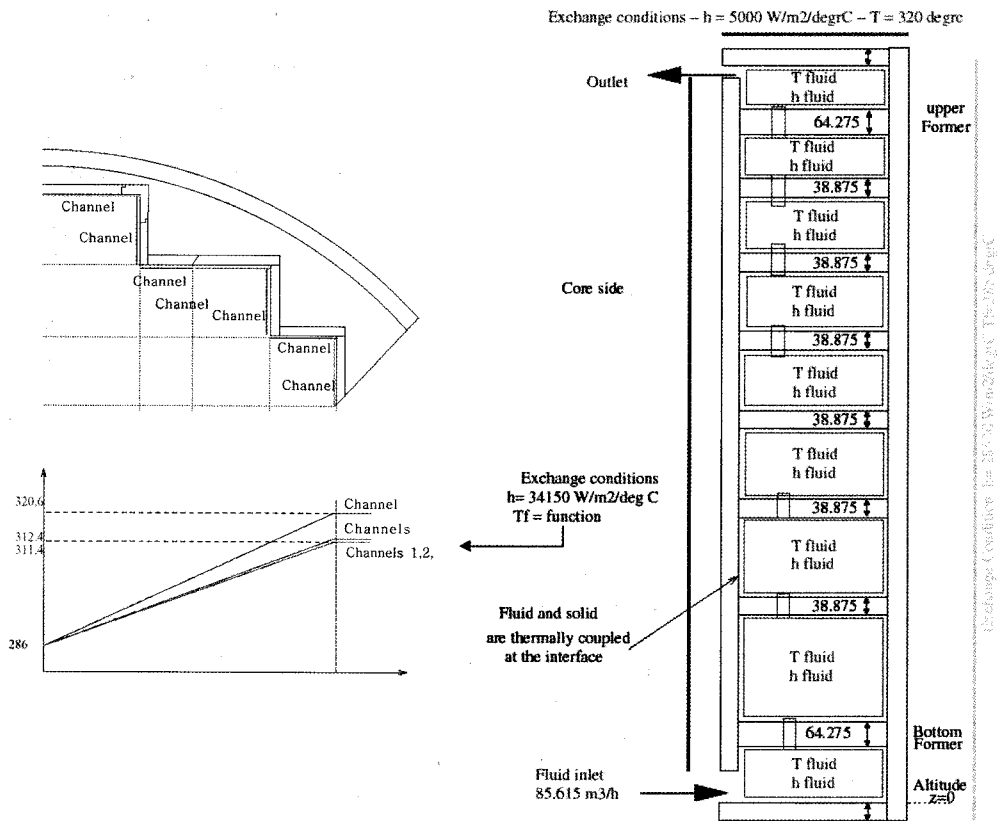


Fig. 5. Summary of the Boundary Conditions used in the Coupled Calculation (Dimensions in mm)

coolant inlet temperature) and $85.615 \text{ m}^3/\text{h}$ (which corresponds to 0.97% of the nominal flow rate). Inlet turbulence quantities are calculated by *Code_Saturne* from the inlet bulk velocity and the hydraulic diameter. A detailed view of the boundary condition set around the head of each bolt is given in the sketch of Figure 4, while the general boundary conditions set are presented in the sketch of Figure 5.

The correlations used on the core side are identical to the ones used for CP0 calculations (see [2]). They have been checked thanks to a CFD calculation that take into account all of the fuel assemblies that are in contact with the core side. It turns out that the heat exchange coefficient retained here is fairly conservative.

The inner cavities walls correspond to a thermally coupled condition between the CFD code and the thermal code.

3.1 Fluid and Solid Meshes Generated

The fluid grid is generated by independent blocks with the grid generator SIMAIL and is mainly composed of bricks and prisms. The number of cells has been kept to its minimum (7 millions) in order not to induce too long a time for calculation. All cooling passages have been taken into account precisely to make sure that the jets are well predicted.

The possibility of *Code_Saturne* to handle non-conforming meshes is used here both to connect the cooling passages to the main cavities and to the depression holes level (see Figure 6).

The solid grid has also been generated in several elementary blocks, as shown in Figure 7. The main difficulty was taking into account both the global structure and geometrical details as fine as the fillet under the head of each bolt. As shown in Figures 8 and 9, the space between the bolts is fairly limited, which can lead to thermal

interaction between the bolts.

On top of geometrical constraints, the solid mesh has to be very fine to capture all of the strong temperature gradients that are potentially present in the core internal baffle structure for several gamma loads. Indeed, if in this paper only a standard fuel arrangement case is presented, calculations for other fuel patterns have been done and are planned in a way to correspond to the variability of the fuel pattern that is observed during the life time of the nuclear plant.

3.2 Heat Source Induced by Gamma Radiation

The heat source calculated by the neutronic Monte-Carlo code TRIPOLI corresponds to a standard fuel arrangement case seen by a French CPY. Figure 10 presents a view of the heat source spatial distribution. As expected, the maximum deposition is located around the corners

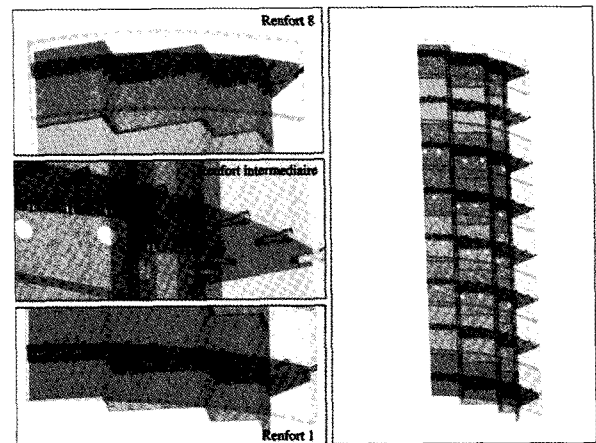


Fig. 7. Global View of the Solid Domain (Including Bolts)

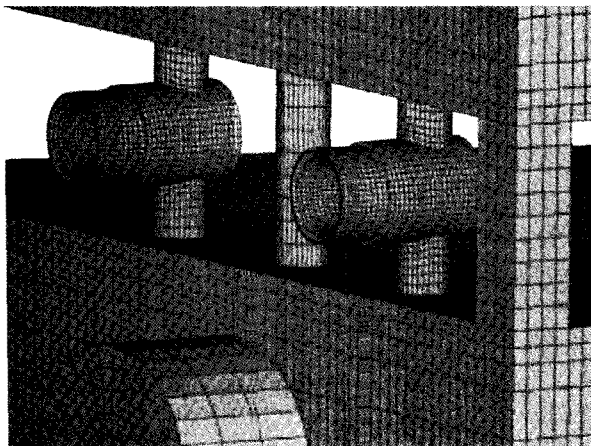


Fig. 6. Geometric Detail of the Fluid Mesh

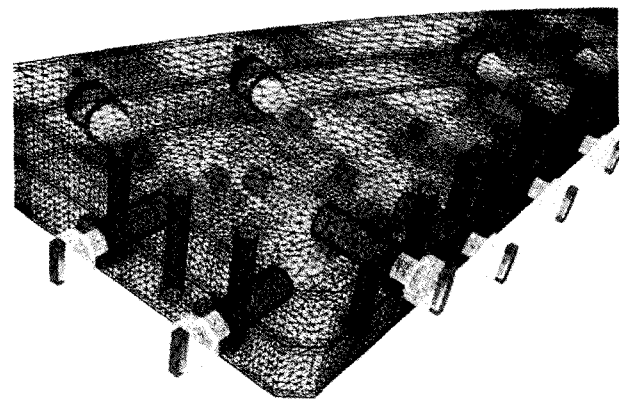


Fig. 8. Detailed View of the Solid mesh (Entering Corner of Former 1)

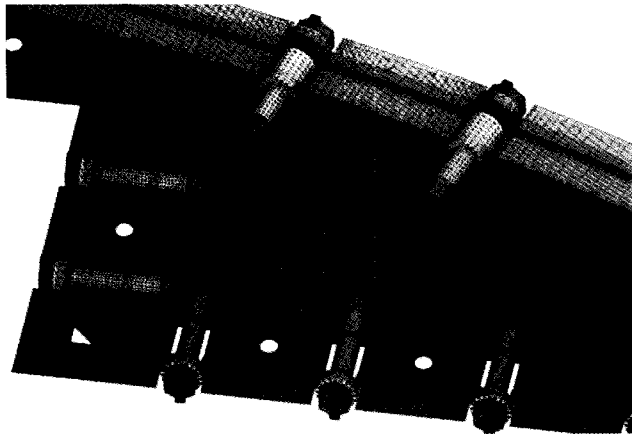


Fig. 9. Horizontal Cut (Middle Plane of Former 2) with Bolts Represented in 3D

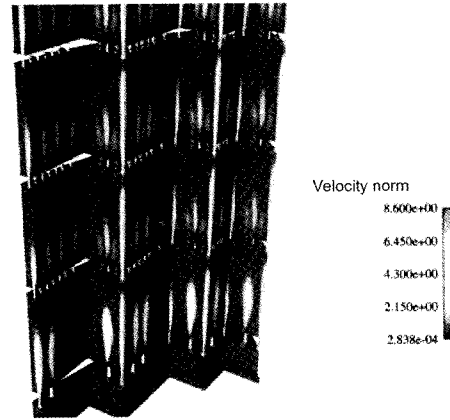


Fig. 11. Velocity Norm Exhibiting the Jets Reattaching to the Baffle Walls (m/s)

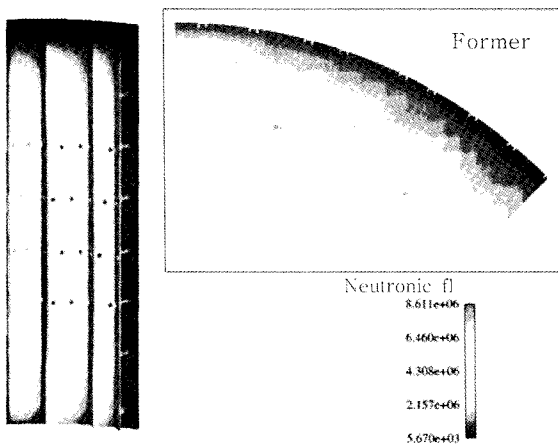


Fig. 10. Heat Source Induced by Gamma Radiation (W/m^3) (Calculated by the Monte Carlo Code TRIPOLI)

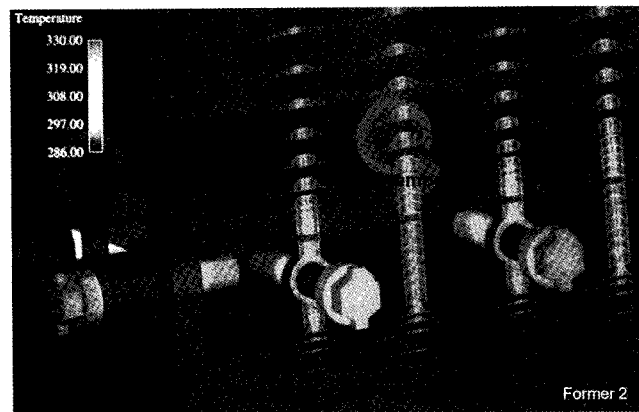


Fig. 12. Detail of the Velocity and Temperature ($^{\circ}C$) Fields through Fluid Cooling Passages

nearest to the core. Values as high as 8.8 MW/m^3 can be encountered in a limited region of the baffle while bolts connected to the barrel (far from the core) see at most 3 MW/m^3 . The deposition inside the water itself has also been estimated (around 0.2 MW/m^3) and has been taken into account in the calculations, but turns out to have very little influence on the fluid temperature, and consequently, on the solid temperature. This is consistent with the observation done in [9].

3.3 CPY Results Discussion

In the present study, we are mainly interested in the steady state reached in nominal conditions, even if both codes have fundamentally non-stationary approaches. Thermal information at the interface is exchanged several hundred times until a converged steady state is obtained both inside the solid and the fluid domains.

The flow is quite complex with multiple eddies created

by the strong jets that were induced by the many holes that bore through the formers and the bolts individual cooling passages. As can be seen in Figure 11, where velocity norm is plotted, jets that correspond to the individual cooling passages have a smaller intensity than those of the simple holes due to stronger head losses. Likewise, one can notice the very strong jet that was induced by the corner channel (present only in the CPY plant). Due to the passages' location (very close to the baffle), all of the jets re-attached the baffle wall quickly, then flowed upwards before being attracted by holes of the next former. One may notice that the first and the last formers are specific where no individual cooling passage is present.

In this calculation, we have assumed that there is no flow through the depressurization holes between the core and the baffle cavities. The velocity field shows a locally small vortex, but this does not influence the global velocity field or the different jets.

Figure 12 shows a detailed view of the velocity and temperature located close to the corner nearest to the core.

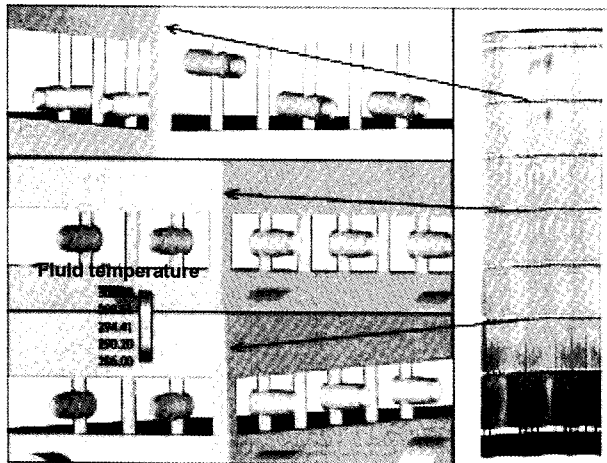


Fig. 13. Fluid Temperature Calculated by *Code_Saturne* (°C)

It also shows the strong cooling of the bolts induced by the flow. One may separate each baffle bolt to 3 regions:

- The first one is the head, where the temperature is influenced by a strong gamma deposition and by the flow located on the core side,
- The second one is the middle part (fillet included) of the bolt, where the temperature is low thanks to the direct cooling,
- The last part is the thread where the temperature is higher, even if the gamma deposition is lower. In this part, there isn't any direct cooling flow.

Figure 13 shows the details of the fluid temperature field near the hottest corner. As expected, the temperature increases as the flow progresses upwards through all of the cavities and gains energy from the surrounding hot walls. However, one has to emphasize that the temperature increase stays moderate (from 286 °C at the inlet up to around 300 °C at the outlet) due to the introduction of corner flows that limit the apparition of a stagnant flow in the hottest regions. Calculations that include the heat deposition induced by gamma radiation inside the water show that the influence of this parameter could almost be neglected (at most a difference of 1 °C to 2 °C at the fluid outlet).

Figure 14 gives an overview of the solid temperature that was reached by the former 3 level, where the highest temperatures are observed. One can see that high temperatures are only present inside the structure and not at the boundaries where cooling is present. The solid temperature of the baffle (seen from the core side) exhibits a vertical layer structure that is clearly related to the boundary conditions set channel by channel (Figure 5). Figure 15 shows the impact of all the jets reattaching themselves to the internal wall of the baffle on the solid structure. One must emphasize that the cooling effect is essentially due to the higher local heat exchange coefficient (which is induced by higher local velocities) rather than

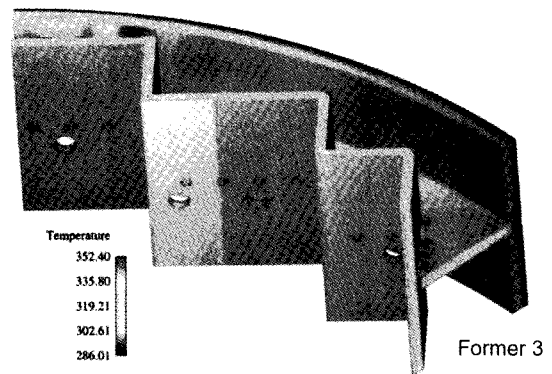


Fig. 14. Wall Temperature at Former 3 (°C) Level

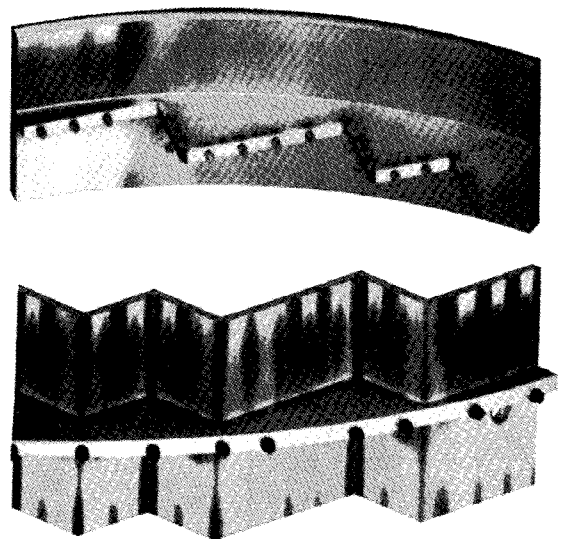


Fig. 15. Wall Temperature at Former 3 (°C) (Core Barrel Removed)

cold temperature. The temperature reached by the bolts at the barrel side is of the same order as the baffle side: there isn't any cooling passage, but the gamma deposition is reduced due to a wider distance from the core.

3.4 Comparisons between CP0 and CPY Design

Figure 16 and Figure 17 present the CPY and CP0 (taken from [2]) horizontal cut plane comparisons (middle plane of the third former) with the same temperature scale.

The maximum temperature found in the CPY is around 252.4 °C compared to about 379 °C. This proves clearly that the new design of the CPY is leading to a lower maximum temperature inside the structure. Regarding the baffle bolts, the difference is even bigger when there is very strong impact from the individual cooling passages. Flow passages through triangular holes located near the entering corner also contribute a lot in the reduction of

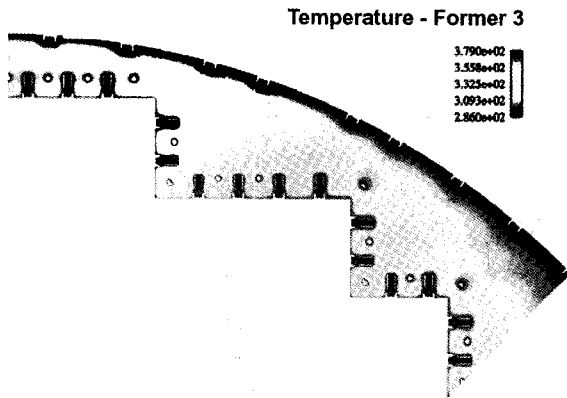


Fig. 16. CPY Wall Temperature (°C) at Former 3 (Core Barrel Removed)

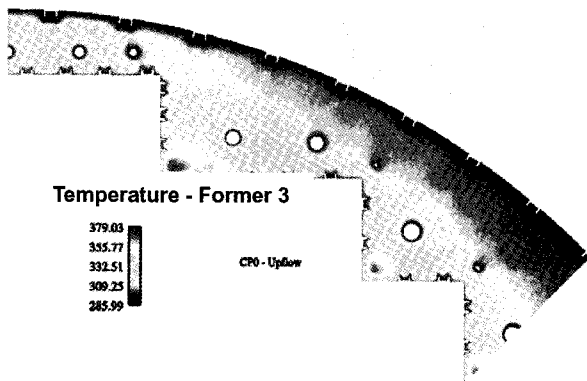


Fig. 17. CP0 Wall Temperature (°C) at Former 3 (Core Barrel Removed)

the temperature level reached by the baffles.

Mechanical studies performed with the two thermal distributions also suggests that the temperature gradients are leading to lower mechanical stresses and are less prone to induce damage. Even though these results constitute the preliminary results, which needs to be confirmed, these results are quite encouraging. On site inspection confirm this trend with almost no problem seen so far on the CPY reactor.

4. TOWARDS HIGH PARALLEL COMPUTATION (HPC) FOR THERMAL PROBLEMS

For the calculations described previously, the CFD code *Code_Saturne* used 192 processors, but SYRTHES was only sequential, and therefore required a processor with a very large memory size (64 Gbytes). Since the completion of these studies, EDF has bought a Blue Gene computer with 8192 processors, but with only 500

Mbytes of memory for each of them. Since the CFD code *Code_Saturne* already has an efficient parallel version, it has been decided to develop a Finite Element thermal code that takes advantage of parallel computers, such as BlueGene.

The approach is fairly classical. It is based on a splitting of the mesh thanks to METIS 5 [10]. METIS is a library that partitions graphs or finite element meshes.

A pre-calculation step is done on a scalar processor that has a large memory of 64 Gbytes to prepare the local mesh tables for exchange. Then, each processor works locally with the local mesh of the part. During the computation phase, elementary matrix and boundary conditions are calculated locally at each time step. The necessary contributions of the surrounding domains are sent via MPI (Message Passing Interface [11]) messages and are added to the local contribution.

The solver is based upon a fairly classical conjugate gradient iterative approach that is preconditioned by the diagonal. Here, the advantage of a simple diagonal preconditioning is its very low cost.

Some assembly operations on the mass matrix are done once l for each time step, which saves memory storage requirements and data transfer between the parts during the iterative steps.

On the other hand, extra-diagonal term contributions need to be added at each level of the conjugate gradient algorithm. That leads to the exchange of information between the nodes that are located at the interface between the parts. Scalar products are done locally and summed in order to obtain the global result.

4.1 Numerical Test on a Large Solid Mesh

In order to numerically test this new parallel version of the thermal code, it was decided to perform a thermal calculation on a full 360° domain. This consists of a purely solid thermal calculation in which the same neutron heat source deposition has been taken into account, as well as the local heat exchange coefficient spatial distribution provided by the previous conjugate heat transfer calculation (performed on a limited 45° angular sector). Here, for this specific test, information was duplicated on the other sectors in order to be able to compute the full 360° case.

This total solid mesh contains around one billion one hundred and nine million tetrahedra. Again, due to limitation in the mesh generator, the mesh was built by blocks that had to be reassembled in a second phase. Due to the very large database, efficient algorithms based on octree approaches were used to join the different meshes and eliminate the common nodes. Besides the files' reading and writing times, the join operation took just a few minutes of CPU time. The complete mesh file has a size of 72 Gbytes. Figure 18 shows the refinement used for the bolts.

Thanks to the METIS 5 partitioner, the mesh was split into sub domains in order to have a nice load balance (about the same number of cells) on each processor. On

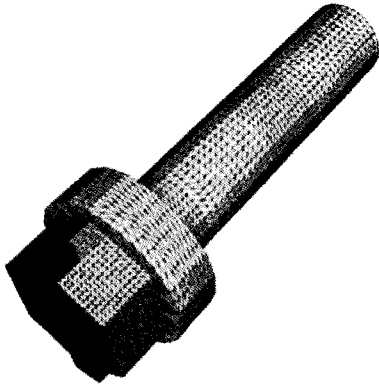


Fig. 18. Detailed View of the Grid used for One Bolt

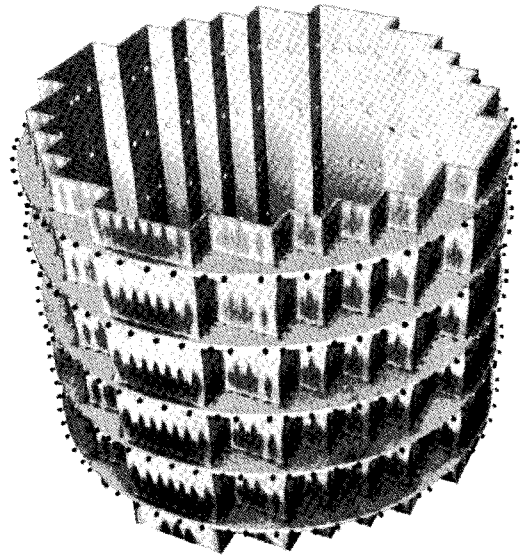


Fig. 20. Temperature Field (Core Barrel Removed)

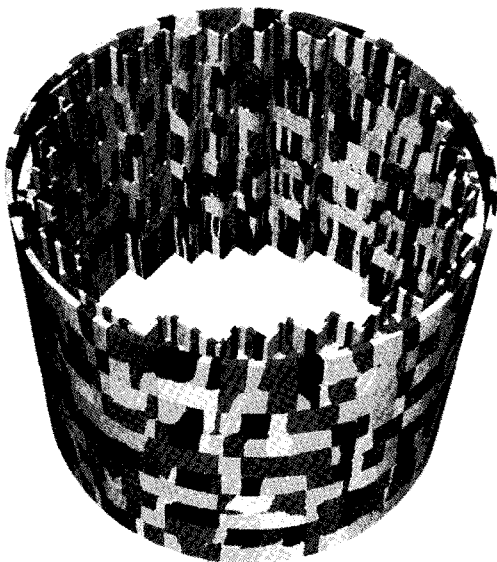


Fig. 19. Decomposition of the 1.1 Billion Cells Mesh in 2048 Parts (Thanks to METIS 5)

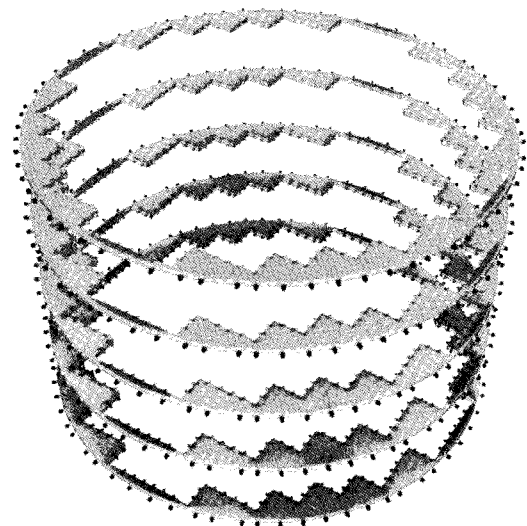


Fig. 21. Only Formers and Bolts are Presented

the scalar preprocessor computer (with 64 Gbytes memory), we however didn't succeed in splitting the complete mesh in one go with METIS 5. On the other hand, there is no problem if the size of the mesh stays under a few tens of million tetrahedra. Here, to overcome this memory limitation, we partitioned each block independently to an adequate number of independent parts, and listed in a specific file which sub-domain each element belonged to. Thus, in the pre-processing step, it was only necessary to read these lists and by-pass the partitioning step.

The preprocessing step (even after memory optimization) and the by-passing of the METIS step still required about 61 Gbytes for 1.1 billion tetrahedra.

For this particular calculation, it was decided to split the total mesh in 2048 parts, which corresponds to a

tradeoff between an easy access to the EDF computer resources, and a fast wall clock time. Figure 19 shows the complete mesh split into 2048 parts. Each part contains around 500 000 elements.

For this particular calculation, the BlueGene did perform nicely without any trouble. It provided a converged state in about 4400 seconds.

Figures 20 to 22 show the temperature fields obtained, which are thankfully very similar (less than 1 °C difference on the maximum temperatures) to what had been obtained in previous calculations done on a sector that was limited to a 45° angle.



Fig. 22. Temperature Field Inside each Bolt

5. CONCLUSIONS AND PERSPECTIVES

This paper presented a numerical approach to address the temperature distribution in the bolts and walls of a core internal baffle structure. This study suggests that the new design adopted for the CPY plants can lead to a reduction in the maximum temperatures of the structures. This is consistent with what has been observed on site where very few cracked bolts have been detected.

Such an industrial study is fairly complex because several numerical codes (neutron radiation code, CFD, thermal code) have to be used and data have to be exchanged. Another aspect is related to the difficulty of taking into account very different geometric scales (up to 5m for the global structure, less than 1mm for the fillet under the head of each bolt where there are hundreds of bolts) and several fuel patterns inducing different strong gradient locations. All of this can lead to a very large mesh size.

The CFD code *Code_Saturne* has been ported on parallel architectures during the last few years and behaves very well on the Blue Gene machine, but the need for conjugate heat transfer calculations requires the thermal solid code SYRTHES to be also run on the same parallel computer.

This present calculation constitutes a first step in the process of adapting the thermal code SYRTHES to HPC calculation on parallel computers for large databases. The coupling between the parallel version of the CFD code *Code_Saturne* and the parallel version of the thermal code SYRTHES is in progress.

One should also emphasize that the grid generation part (at least with classical commercial software) is becoming more and more the bottleneck for such industrial studies.

ACKNOWLEDGMENTS

The authors would like to particularly thank E. Quemerais (INCKA) for the generation of the elementary pieces of

the meshes with the mesh-generator SIMAIL, and Y. Fournier and M. Sakiz (EDF R&D) for helpful discussions regarding the use of *Code_Saturne*.

NOMENCLATURE

ρ	density
U_i	velocity component
p^*	pressure
g	gravity
x_i	coordinates
t	time
μ	viscosity
C_p	specific heat
k_s	thermal conductivity
ϕ	volume heat source
h	heat transfer coefficient
T	temperature

REFERENCES

- [1] C. POKOR, Y. THEBAULT, C. PUJOL, E. LEMAIRE, N. LIGNEAU "Metallurgical Examination Update of Baffle Bolts Removed from Operating French PWR" *Proc. of the International Symposium Fontevraud VI*, SFEN, 2006.
- [2] C. PENIGUEL, I. RUPP, N. LIGNEAU, M. TOMMY-MARTIN, L. BELOEIL, E. LEMAIRE "Thermal Analysis of a PWR core internal baffle structure" - *Proceeding PVP 2006*, Vancouver, Canada.
- [3] *Code_Saturne* documentation "Code_Saturne 1.4.0 Theory and Programmer's Guide" <http://www.code-saturne.org>.
- [4] F. ARCHAMBEAU et al, "Qualification of *Code_Saturne* for thermal hydraulics Single Phase Nuclear Applications". - *Super Computing Nuclear Applications Conference*, Paris, France 2003.
- [5] J.H. FERZIGER, M. PERIC, "Computational Methods for Fluid Flow Dynamics". Springer, third Edition (2002).
- [6] C.M. RHIE, W.L. CHOW, "A numerical study of a turbulent flow past an isolated airfoil with training edge separation", *AIAA* paper, 82-0998.
- [7] I. RUPP and C. PENIGUEL, "Coupling heat conduction radiation and convection in complex geometries". *Int Journal of Numerical Methods in complex geometries, Methods for Heat and fluid Flow* Vol. 9, University Press, 1999.
- [8] C. PENIGUEL, I. RUPP, "Coupling heat conduction, radiation and convection phenomena in complex 2D and 3D geometries", *Proceeding Numerical methods in thermal problems*, Swansea, 1997.
- [9] Y.K. LEE, J.C. DAVID, H. CARCREFF "A gamma heating calculation methodology for research reactor" - *RRFM 2001 - 5th International topical meeting on research reactor fuel management* - p 147-151 - European Nuclear Society, Berne, Switzerland.
- [10] G. KARYPIS, V. KUMAR "A fast and high quality multilevel scheme for partitioning irregular graphs", *SIAM Journal of Scientific Computing*, Vol 20, No. 1, pp. 359-392, 1999.
- [11] "MPI : A Message-Passing Interface Standard - Version 2.1" - 2008 - <http://www.mpi-forum.org/docs/docs.html>, <http://www.mcs.anl.gov/research/projects>